JOURNAL OF THE AMERICAN CHEMICAL SOCIETY

Subscriber access provided by UNIV OF SOUTHERN QUEENSLAND

Article

Chiral Substituted Poly-N-vinylpyrrolidinones and Bimetallic Nanoclusters in Catalytic Asymmetric Oxidation Reactions

Bo Hao, Medha J. Gunaratna, Man Zhang, Sahani Weerasekara, Sarah N. Seiwald, Vu T. Nguyen, Alex Meier, and Duy H. Hua

J. Am. Chem. Soc., **Just Accepted Manuscript** • DOI: 10.1021/jacs.6b12113 • Publication Date (Web): 05 Dec 2016

Downloaded from http://pubs.acs.org on December 5, 2016

Just Accepted

"Just Accepted" manuscripts have been peer-reviewed and accepted for publication. They are posted online prior to technical editing, formatting for publication and author proofing. The American Chemical Society provides "Just Accepted" as a free service to the research community to expedite the dissemination of scientific material as soon as possible after acceptance. "Just Accepted" manuscripts appear in full in PDF format accompanied by an HTML abstract. "Just Accepted" manuscripts have been fully peer reviewed, but should not be considered the official version of record. They are accessible to all readers and citable by the Digital Object Identifier (DOI®). "Just Accepted" is an optional service offered to authors. Therefore, the "Just Accepted" Web site may not include all articles that will be published in the journal. After a manuscript is technically edited and formatted, it will be removed from the "Just Accepted" Web site and published as an ASAP article. Note that technical editing may introduce minor changes to the manuscript text and/or graphics which could affect content, and all legal disclaimers and ethical guidelines that apply to the journal pertain. ACS cannot be held responsible for errors or consequences arising from the use of information contained in these "Just Accepted" manuscripts.

ACS Publications

Journal of the American Chemical Society is published by the American Chemical Society. 1155 Sixteenth Street N.W., Washington, DC 20036
Published by American Chemical Society. Copyright © American Chemical Society. However, no copyright claim is made to original U.S. Government works, or works produced by employees of any Commonwealth realm Crown government in the course of their duties.

Chiral Substituted Poly-*N*-vinylpyrrolidinones and Bimetallic Nanoclusters in Catalytic Asymmetric Oxidation Reactions

Bo Hao, Medha J. Gunaratna, Man Zhang, Sahani Weerasekara, Sarah N. Seiwald, Vu T. Nguyen, Alex Meier, and Duy H. Hua*

Department of Chemistry, Kansas State University, Manhattan, KS 66506 USA

KEYWORDS: catalytic asymmetric C-H oxidation, catalytic asymmetric oxidations of diols and alkenes, chiral substituted poly-N-vinylpyrrolidinones, Cu/Au, nanoclusters, Pd/Au.

ABSTRACT: A new class of poly-*N*-vinylpyrrolidinones containing an asymmetric center at C5 of the pyrrolidinone ring were synthesized from L-amino acids. The polymers, particularly **17**, were used to stabilize nanoclusters such as Pd/Au for the catalytic asymmetric oxidations of 1,3- and 1,2-cycloalkanediols and alkenes, and Cu/Au for C-H oxidation of cycloalkanes. It was found that the bulkier the C5 substituent in the pyrrolidinone ring, the greater the optical yields produced. Both oxidative kinetic resolution of (±)-1,3- and 1,2-*trans*-cycloalkanediols and desymmetrization of meso *cis*-diols took place with 0.15 mol% of Pd/Au (3:1)-**17** under oxygen atmosphere in water to give excellent chemical and optical yields of (*S*)-hydroxy ketones. Various alkenes were oxidized with 0.5 mol% of Pd/Au (3:1)-**17** under 30 psi. of oxygen in water to give the dihydroxylated products in >93% ee. Oxidation of (*R*)-limonene at 25°C occurred at the C-1,2-cyclic alkene function yielding (1*S*,2*R*,4*R*)-dihydroxylimonene **49** in 92% yield. Importantly, cycloalkanes were oxidized with 1 mol% of Cu/Au (3:1)-**17** and 30% H_2O_2 in acetonitrile to afford chiral ketones in very good to excellent chemical and optical yields. Alkene function was not oxidized under the reaction conditions. Mechanisms were proposed for the oxidation reactions and observed stereo- and regio-chemistry were summarized.

INTRODUCTION

Bimetallic nanoclusters which comprised of two metals have distinct properties from those comprised of single metals and bulk molecules. For this reason, they have attracted great interest in recent years.[1,2] However, asymmetric oxidations of diols, alkenes, and cycloalkanes using bimetallic nanoclusters have not yet been reported previously.

In Au-bimetallic nanoclusters, such as Pd/Au, it has been suggested that Au pulls electron density from Pd leading to a greater interaction of $Pd^{(\delta+)}$ with the substrates.[3,4] Nanoclusters are generally stabilized by inorganic oxides, glutathione,[5] or organic polymers including poly-*N*-vinylpyrrolidinone (PVP),[3] poly(amidoamine) (PAMAM),[6] chitosan,[7] and others,[8] which prevent the nanoparticles from aggregation and oxidation.[9] The use of chiral polymers as chiral inducers with bimetallic nanoclusters in the catalytic asymmetric oxidation reactions is unprecedented.

Organic transformation reactions of bimetallic nanoclusters[1] in the oxidation of alcohols,[3,10,11] formic acid oxidation,[12] aldehyde oxidation,[13] oxidation of tetralin,[14] Ullmann coupling,[15] Suzuki coupling reaction,[16] tandem oxidation-Michael addition reaction,[17] have been reported. However, these reports do not include studies of enantio- or stereo-selectivity. Although desymmetrization of meso diols and diol derivatives using various organic reagents and enzymes have appeared,[18-21] reports on the enantioselective oxidation of a mixture of racemic diols via kinetic resolution are limited, with the exception of oxidation of racemic benzylic vicinal diols.[22] Hence, asymmetric oxidation of racemic or meso diols using bimetallic nanoclusters and chiral stabilizer may shed light onto the chemistry of the stabilizer and enhance the synthetic applicability of the method.

Catalytic asymmetric syn-dihydroxylation reactions have been intensely pursued, and the Sharpless asymmetric dihydroxylation process is a major breakthrough in asymmetric catalysis.[23] However, there are a few shortfalls in the methodology and they include: a lower enantioselectivity in some *Z*-1,2-disubstituted alkenes, alkenes containing stereogenic centers, and the toxicity and volatility of osmium tetraoxide catalyst.[23] Various improvements on the enantioselectivity of syn-dihydroxylation using osmium as catalyst have been made.[24,25] Other asymmetric dihydroxylation reactions with osmium-free catalysts[26] including palladium-catalyzed difunctionalization of alkenes,[27] RuO_4,[28] $KMnO_4$,[29] and iron complexes[30] have also been investigated. Asymmetric syn- and anti-dihydroxylation of alkenes using bimetallic nanoparticles and chiral polymers have not been disclosed previously. Avoidance of the use of toxic osmium metal and improving the enantioselectivity in the oxidation of alkenes would advance the asymmetric synthesis of diols from alkenes.

Regio- and enantioselective C-H oxidation of cycloalkanes is one of the most challenging transformations in organic synthesis. The preferred C-H oxidative sites often took place because of the weaker C-H bond dissociation energy, through-bond electronic effect, steric effect, conjugation and

ACS Paragon Plus Environment

hyperconjugation, and releasing strain.[31] The uses of homogeneous catalysts such as iron complexes,[32-34] gold reagents,[35] and others[31,36-38] in C-H oxidation have appeared. Due to various possible reactive sites in even medium-size organic molecules, the regio- and enantio-selective C-H oxidations inevitably require directing or activating groups such as heteroatoms and allylic moiety.[39-41] Although simple C-H oxidation of cyclohexane with Au nanoclusters on hydroxyapatite support[42] or with Pt/TiO_2[43] has been studied, no reports on the use of bimetallic nanoclusters and chiral supports in the catalytic asymmetric C-H oxidation have surfaced. C-H oxidation is a highly atom-economic process, and regioselective catalytic asymmetric C-H oxidation would provide a powerful tool for organic synthesis.

We report herein the synthesis of a class of chiral substituted poly-*N*-vinylpyrrolidinones (CSPVP) and their chiral induction by chelating Pd/Au or Cu/Au nanoclusters in enantioselective oxidation reactions of diols, alkenes, and cycloalkanes.

RESULTS AND DISCUSSION.

In the reported study of Pd/PVP nanoparticles using extended X-ray absorption fine structure spectroscopy, it has been suggested that the amide function of PVP chelated with Pd and stabilized the nanoparticles.[14,44] We hypothesize that in the complex of substituted PVP and nanoparticles, a substituent on the pyrrolidinone ring would affect the stereochemical outcome of the reactions, resulting in asymmetric oxidations.

Synthesis of Chiral Substituted Poly-*N*-vinylpyrrolidinones (CSPVPs or substituted PVPs containing an asymmetric center). To investigate the effects of the polymers on the bimetallic nanoparticles in oxidation reactions, we synthesized four CSPVPs **15** - **18** from optically pure amino acids (Scheme 1) and utilized them as stabilizers in the asymmetric oxidation reactions. Our synthesis of CSPVPs started from the polymerization of chiral 5-substituted *N*-vinylpyrrolidinones **9** – **11**, which were prepared from the vinylation of the corresponding 5-substituted-2-pyrrolidinones, **6** – **8**, respectively. Chiral **6** - **8** were made from L-amino acids by following a reported procedure.[45-47] Hence, *N*-Boc L-(*S*)-amino acids, **1** and **2**, were separately coupled with Meldrum's acid followed by reduction of the ketone function with sodium borohydride, cyclization under heat,[45] and removal of the Boc group with trifluoroacetic acid (TFA) in CH_2Cl_2 to give **5** and **7**, respectively. The *N*-Boc protecting group of **3** can be removed selectively in the presence of *O*-*tert*-butyl group by TFA/CH_2Cl_2 at 25°C providing **6**. From our studies (*vide infra*), it appears that a bulky substituent at C5 of the polymer would afford a higher enantioselectivity. Consequently, (*R*)-5-benzhydryloxymethyl-2-pyrrolidinone (**8**) was synthesized from the alkylation of compound **5** with sodium hydride and benzhydryl bromide. *N*-Vinylation of **6** – **8** with Na_2PdCl_4 and vinyl acetate[48] gave the corresponding *N*-vinylpyrrolidinones **9** - **11**, respectively.

To prepare uniform micron-size monodisperse particles,[49] we utilized a dispersion polymerization method[50] to prepare polymers **15** – **17** (Scheme 1). The dispersants, poly(5-substituted *N*-vinylpyrrolidinone-co-vinyl acetate) **12** – **14** were prepared from the copolymerization reactions of respective monomers **9** – **11** and 1 equiv. of vinyl acetate in the presence of a catalytic amount of azobisisobutyronitrile (AIBN) in refluxing acetone. Polymerization of **9** – **11** separately with a catalytic amount of AIBN and in the presence of 1% of respective copolymer **12** – **14** in DMF at 120°C for 7 days gave polymers **15** – **17**. Polymer **18** was prepared through the removal of the *tert*-butyl group of polymer **15** with TFA. Polymers **15** - **18** are soluble in water and their molecular weights were determined by gel permeation chromatography [see Figure S1 in Supporting Information (SI)]. Average molecular weights of **15** - **18** are listed (Scheme 1). Both *R*- and *S*-stereochemistry are likely presented in the stereogenic center (marked with *) in the polymer alkane backbone, and they are not identifiable. Presumably, this stereogenic center of the polymers can be isotactic, atactic, and syndiotactic,[51] and likely has lesser effect on the asymmetric oxidation reactions. The average sizes, size distribution, and shapes of the polymers were also studied by atomic force microscopy (AFM) and dynamic light scattering (DLS). AFM images of the polymers such as **17** in aqueous solution showed spheroid and ellipsoid shapes with diameter ~20 - 30 nm (Figures S2A-S2B). DLS graphs of **17** showed a major ensemble of 12 – 20 nm sizes particles with an average size of 18.6 nm along with a few 152 nm-sized particles, suggesting that different shapes and few large aggregates were presented in the aqueous solution (Figures S3A - S3B). On the contrary, nanoclusters Pd/Au-**17** showed more discrete sizes in solution by DLS (*vide infra*).

Synthesis of Bimetallic Nanoclusters-CSPVP. Nanoclusters can be prepared by a number of methods including molecular beams, chemical reduction, thermal decomposition, ion implantation, electrochemical synthesis, radiolysis, sonochemical synthesis, and biosynthesis, and are characterized by various analytical techniques.[52] We have synthesized various bimetallic nanoclusters including Pd/Au and Cu/Au, using the chemical reduction method[3] in the presence of chiral polymer **15**, **16**, **17**, or **18**. We used gold due to its high catalytic activity and synergistic electronic effects.[3-9] For example, a solution of Na_2PdCl_4 (3 equiv.), $HAuCl_4$ (1 equiv.), and CSPVP **17** (0.11 equiv.; based on the amount of Au) in water was treated with $NaBH_4$ at 25°C for 30 min (Scheme 1) to give a light brown to dark grey solution depending on the concentrations (Figure S4). The resulting solution was used in the subsequent catalytic reactions without further manipulation. Similarly, Cu/Au (3:1)-**17** was also prepared using CuCl (3 equiv.), $HAuCl_4$ (1 equiv.), and CSPVP **17** (0.11 equiv.). The aforementioned nanocluster solution was filtered through a Vivaspin 20 centrifugal filter device (3,000 MWCO), washed with deionized water twice, and lyophilized to give a powder, which was used for various characterization including inductively coupled plasma-mass spectrometry (ICP-MS; see SI), transmission electron microscopy (TEM; Figure S5), X-ray photoelectron spectroscopy (XPS; Figure S6), AFM (Figures S2C - S2D), DLS (Figures S3C - S3D), and IR. Results of the ICP-MS showed a ratio of 3.12 ± 0.58 of Pd and Au in the Pd/Au (3:1)-**17** complex, and a ratio of 3.0 ± 0.4 of Cu and Au in the Cu/Au (3:1)-**17** sample. This is in agreement of the 3:1 ratio of the two metals used in preparation of the nanoclusters. TEM images revealed average diameters of 3.44 ± 1.63 nm and 3.66 ± 1.95 nm for Pd/Au (3:1)-**17** and Cu/Au (3:1)-**17**, respectively (Figure S5). The nano-sizes (2 - 4 nm) of the nanoclusters are similar to those reported for Pd/Au using PVP as a stabilizer.[3,14] XPS spectra of the Pd/Au (3:1)-**17** showed the binding energies of 84.1 eV and 335.1 eV derived from $4f_{7/2}$ Au and $3d_{5/2}$ Pd, respectively (Figure S6).[14] The spectra of Cu/Au (3:1)-**17** displayed binding energies of 84.1 eV and 932.7 eV for respective $4f_{7/2}$ Au and $2p_{3/2}$ Cu (Figure S6). The binding energy values are consistent with those reported in the

XPS database. From the AFM images of Pd/Au (3:1)-**17**, 50 – 200 nm in diameters and ~5.8 nm in heights of spherical particles were found, and in DLS, 100 – 140 nm sized nanoparticles were revealed (Figure S2C, 2D), suggesting the size of polymer **17** wrapped particles was ~5 times larger than polymer **17** alone, and the measured sizes of the polymer-particles from AFM and DLS were similar. As reported previously, AFM does not resolve subtle shape differences from the diameters, but can provide relatively accurate height of the nanoparticles.[53] The ~5.8-nm height revealed by AFM is similar to that found by TEM. A small amount of ~15.7 nm-sized particles found in DLS of Pd/Au-**17** sample may derive from free polymer **17** without complexing Pd/Au in the aqueous solution. The approximate total numbers of metal atoms and molecules of polymer in a spherical nanocluster can be calculated utilizing the magic-cluster sizes $N_{total} = 1/3\ (10n^3 - 15n^2 + 11n - 3)$, where n is the number of layers of shell in the metallic nanoparticles with face-centered cubic close-packed structure.[54] Since the average sizes of Pd/Au (3:1)-**17** and Cu/Au (3:1)-**17** nanoclusters are 3.44 and 3.66 nm, respectively (from TEM), there are respectively ~727 and 1,151 atoms of Pd/Au (3:1) and Cu/Au (3:1) in a nanocluster calculating from the aforementioned equation and particle sizes (see SI for calculation). Each Pd/Au and Cu/Au nanoclusters are stabilized by approximately 20 and 32 molecules of polymers, respectively (see SI).[4] Because of the numbers of molecules and extended structure of the chiral polymer, the sizes of the bimetallic nanocluster/polymer found by AFM and DLS are much larger than those in the nanoclusters found by TEM (the polymer cannot be observed by TEM). The amide C=O

Scheme 1. Syntheses of poly-*N*-vinylpyrrolidinones containing an asymmetric center at C5 and preparations of Pd/Au (3:1)-**17** and Cu/Au (3:1)-**17**.

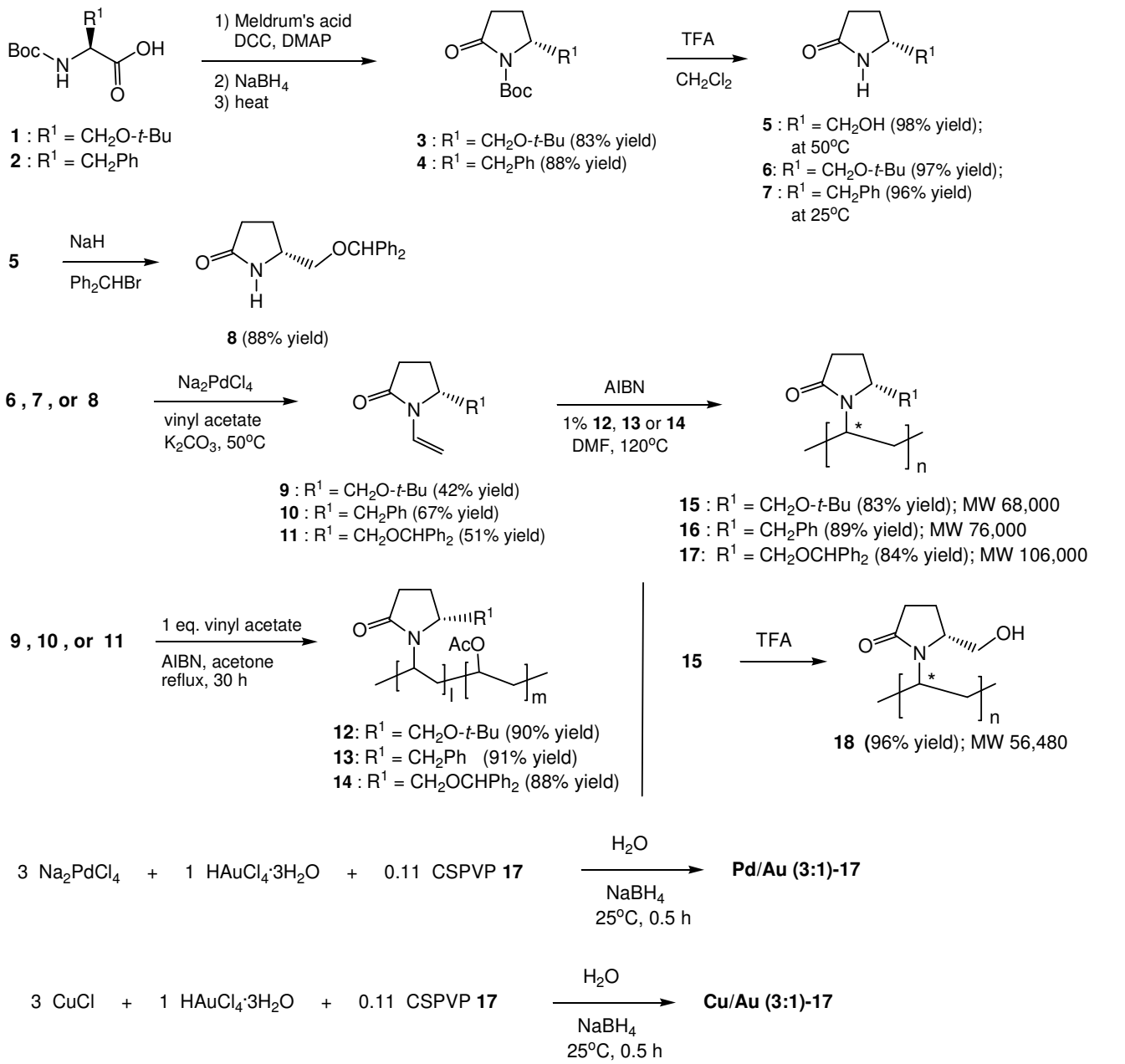

absorption band of the pyrrolidinone ring at 1650 cm^{-1} of polymer **17** in IR spectrum shifted to 1641 cm^{-1} for Pd/Au (3:1)-**17**, implying a greater character of $^{\delta-}O-C=N^{\delta+}$ of the amide group in the nanoclusters due to chelation with the metals.

Catalytic asymmetric oxidation of cycloalkanediols.

After screening different ratios of Pd versus Au such as 1:1, 2:1, 3:1 of the bimetallic nanoclusters, Pd/Au (3:1)-CSPVP appears to provide the highest catalytic activity and chemical yields[3] in the aerobic catalytic asymmetric oxidation of cycloalkanediols. Initially, (±)-*trans*-1,3-cyclohexanediol (**20**) was used to screen the enantioselectivity of various CSPVPs such as **15** – **18**, and results are summarized in **Table 1**. For instance, treatment of (±)-**20** with 0.15 mol% of Pd/Au (3:1)-CSPVP **15**, **16**, **17**, or **18** (the amount of catalyst is based on the total moles of Pd and Au) and 0.3 equiv of K_2CO_3 in water under 1 atmospheric oxygen at 60°C for 7 days gave 46 – 49% chemical yields [or 92 – 97.5% yields based on reacted (*S*,*S*)-**20**] and 70 - 99% ee optical yields of (*S*)-3-hydroxycyclohexanone (**23**) along with the recovered (*R*,*R*)-**20** (**Table 1**, entries 1 – 4). Results suggest that a bulkier C5-substituent on the pyrrolidinone ring of the polymer provided a greater optical yield. Since polymer **17** provided the highest chemical and optical yields, it was used for all other oxidation reactions including oxidations of alkenes and cycloalkanes. Diol (*R*,*R*)-**20** was recovered in 50% yield and 92% ee from the reaction with Pd/Au (3:1)-**17**, suggesting that it reacted much slower than (*S*,*S*)-**20** under the reaction conditions, i.e., a kinetic resolution is resulted. Hydroxyl ketone (*S*)-**23** did not undergo oxidation, revealing an electron-withdrawing ketone group impeded further oxidation. The rate of the oxidation reaction was enhanced in the presence of 0.3 equiv of K_2CO_3. Using 0.15 mol% of Pd/Au (3:1)-**17**, other five- and seven-membered cycloalkanes, such as 1,3-*trans* diols (±)-**19** and (±)-**21** and 1,2-*trans* diols (±)-**28** - (±)-**30**, were similarly oxidized to give excellent chemical and optical yields. Results are presented in **Table 1** (entries 5 and 6, and entries 10 - 12). When the amounts of catalysts were increased to 0.30 mol% (double) or 0.60 mol% (quadruple) of Pd/Au (3:1)-**17**, the oxidations of (±)-**20** were respectively completed in 6 and 5 days, with chemical yields of 47% (99% ee) and 49% (99% ee) of (*S*)-**23**. Hence, an increase of the amounts of catalyst shortens the reaction time. Oxidation of (±)-**20** with 0.15 mol% of Pd-**17** without Au under similar

Table 1. Catalytic asymmetric oxidation of 1,3-diols and 1,2-diols.

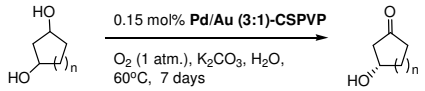

entry	substrate	CSPVP	product	% yield[a]	% ee	recovered diol	% yield[b]	% ee
1	(±)-**20**	**15**	(S)-**23**	46	83	(*R*,*R*)-**20**	52	79
2	(±)-**20**	**16**	(S)-**23**	47	88	(*R*,*R*)-**20**	52	81
3	(±)-**20**	**17**	(S)-**23**	49	99	(*R*,*R*)-**20**	50	92
4	(±)-**20**	**18**	(S)-**23**	46	70	(*R*,*R*)-**20**	51	65
5	(±)-**19**	**17**	(*S*)-**22**	48	99	(*R*,*R*)-**19**	53	91
6	(±)-**21**	**17**	(*S*)-**24**	46	99	(*R*,*R*)-**21**	53	85
7[c]	**25**	**17**	(*S*)-**22**	97	90	-	-	-
8[c]	**26**	**17**	(S)-**23**	89	91	-	-	-
9[c]	**27**	**17**	(*S*)-**24**	95	92	-	-	-

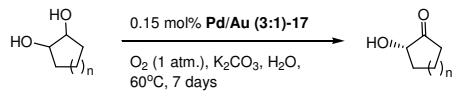

entry	substrate	CSPVP	product	% yield[a]	% ee	recovered diol	% yield[b]	% ee
10	(±)-**28**	**17**	(*S*)-**31**	47	99	(*R*,*R*)-**28**	50	88
11	(±)-**29**	**17**	(S)-**32**	45	99	(*R*,*R*)-**29**	50	87
12	(±)-**30**	**17**	(*S*)-**33**	47	99	(*R*,*R*)-**30**	54	88
13[c]	**34**	**17**	(*S*)-**31**	94	91	-	-	-
14[c]	**35**	**17**	(S)-**32**	97	92	-	-	-
15[c]	**36**	**17**	(*S*)-**33**	94	91	-	-	-

(a) Isolated yields were based on starting racemic or meso-diols. (b) Percent recoveries were based on recovered unreacted starting diols. (c) Reactions were carried out at 120°C under 30 psi. of oxygen for 3 days.

reaction conditions (at 60°C for 7 days) gave only 29% yield of (*S*)-**23** in 95% ee, indicating bimetallic Pd/Au provided higher chemical and optical yields in the catalytic oxidation reactions. Catalyst Au-**17** alone gave no oxidized product. When the temperature of the reaction was increased from 60°C to 80°C, the rate of the reaction did not change (7 days and 47% yield was found), whereas the optical yield of (*S*)-**23** decreased to 94% ee. Further increasing the temperature to 100°C resulted

in completion of the reaction in 6 days with a 47% yield of (*S*)-**23** in 89% ee, indicating that higher reaction temperature lowers the optical yield. The recyclability of the Pd/Au (3:1)-**17** catalyst was also examined. Hence, the catalyst, recovered from the oxidation reaction of (±)-**20**, was reused under similar reaction conditions for a second time, and 39% yield (99% ee) of (*S*)-**23** was isolated. The catalyst was further recycled for a third time, but only 18% yield (98% ee) of (*S*)-**23** was obtained, showing the catalyst can be reused albeit with lower catalytic activities. The turnover number (TON) of the catalytic oxidation reaction after three cycles is 706 (SI). The absolute configurations of (*S*)-**22**, (*S*)-**23** and (*S*)-**31** – (*S*)-**33** were determined by comparison of the sign of the reported specific rotations (see SI).[55-58] Optical purities were measured through HPLC/chiral column of their benzoyl derivatives, which were synthesized by the treatment of the hydroxyl ketones with benzoyl chloride and pyridine (SI). In all cases, PVP was used in place of CSPVP under similar reaction conditions to provide the racemic products for HPLC/chiral column analyses. The selectivity factor values of the HPLC/chiral column separation are 1.10 – 1.28 (see Table S1 in SI), indicating an acceptable separation. The specific rotation of (*S*)-**24** has not been reported previously and its absolute configuration was assumed based on the retention time of its benzoate derivative in HPLC/chiral column. The (*R*)-enantiomer has a lower retention time than that of (*S*)-enantiomer, which is in agreement with benzoate derivatives of (*S*)-**22** and (*S*)-**23** (see SI). The absolute configurations and optical purities of the unreacted diols (*R*,*R*)-**19** – (*R*,*R*)-**21** and (*R*,*R*)-**28** – (*R*,*R*)-**30** were similarly determined by comparison of the sign of the reported specific rotations[59,60] (SI) and through HPLC/chiral column of their dibenzoate derivatives obtained from the reactions of the diols with benzoyl chloride and pyridine (SI).

To our surprise, the meso 1,3-*cis* and 1,2-*cis*-cycloalkanediols did not undergo oxidation reactions under similar reaction conditions as those of *trans*-diols. It may due to the fact that *cis*-diols form stable complexes with the nanoparticles.[61] However, under elevated pressure of oxygen (30 psi.) and temperature (120°C), the reactions took place in 3 days to give 89 – 97% yields and 90 – 92% ee of the oxidized (*S*)-hydroxyl ketones

Scheme 2. **Proposed mechanism and oxidative sites for the catalytic asymmetric oxidation of racemic and meso 1,3- and 1,2-diols**.

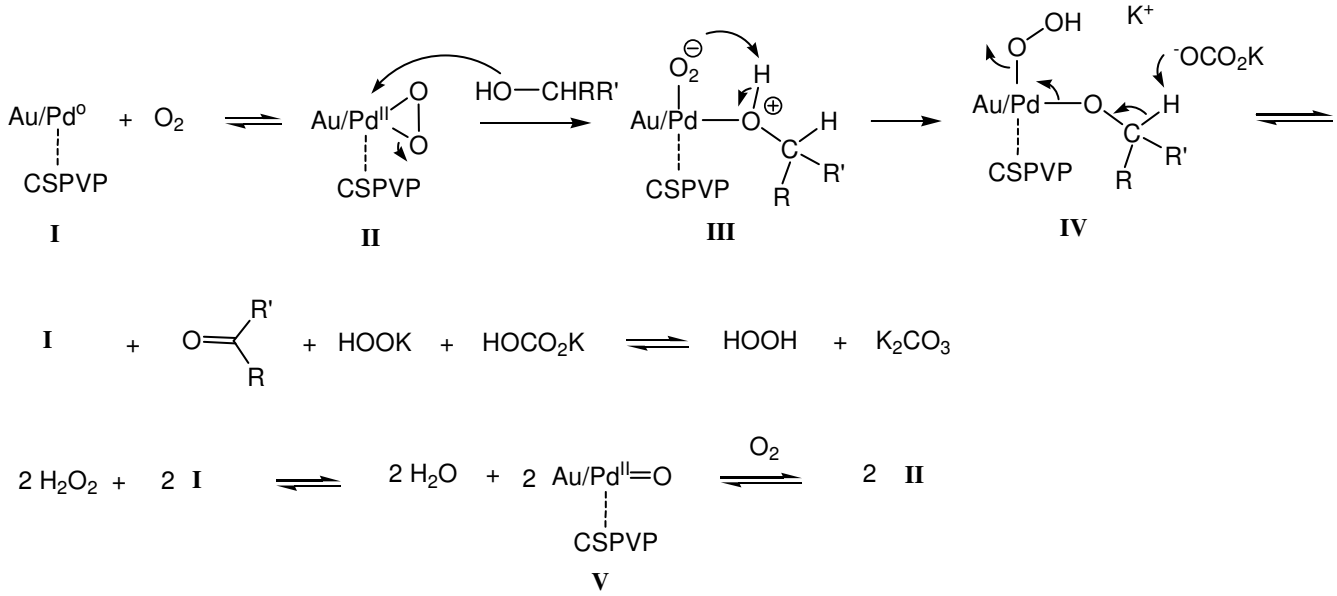

Oxidative sites for racemic **1,3- and 1,2-*trans*-diols** leading to (*S*)-hydroxy ketones:

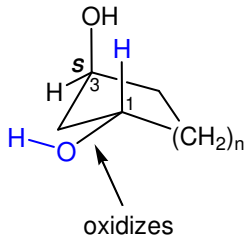

VIa (n = 1 - 3)

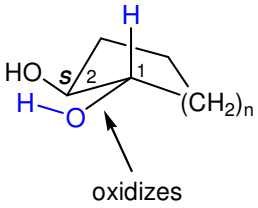

VIb (n = 1 - 3)

Oxidative sites for meso **1,3- and 1,2-*cis*-diols** leading to (*S*)-hydroxy ketones:

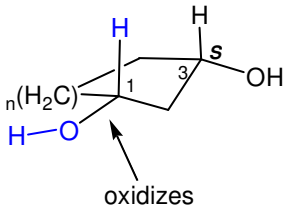

VIIa (n = 1 - 3)

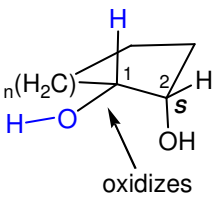

VIIb (n = 1 - 3)

(**Table 1**, entries 7 – 9 and entries 13 – 15). The higher reaction temperature (120°C) lowers the optical yields in the catalytic oxidation reactions. No changes in reaction rate and chemical and optical yields in the oxidation reaction of meso-**35** were found when doubling the amount of **17** but maintaining the same amount of Pd/Au (3:1; 0.15 mol%). This

oxidative desymmetrization of meso-diols is synthetically useful, since it provides the chiral hydroxyketones without the recovery of starting diols. Importantly, both *trans*- and *cis*-diols gave only the (*S*)-hydroxy ketones.

Scheme 2 outlined a proposed mechanism and oxidative sites for the enantioselective oxidation reactions of diols. A η^2-peroxido Pd^{II} (peroxopalladium) species **II**[62] may form similar to that reported.[63] A diol such as (*S*,*S*)-**20** attacks Pd of **II** leading to complex **III**, which undergoes proton transfer to give **IV**. Subsequent removal of C1-H by K_2CO_3 leads to (*S*)-**23** and **I** and hydrogen peroxide. Presumably, the C5(*R*)-bulky substituent of pyrrolidinone ring directs the stereo- and regio-chemistry of the oxidation reactions. The oxidative sites in *trans*- and *cis*-diols are depicted in **VI** and **VII**, respectively.

The pro-*S*-configurated carbon center of *trans*-diols (1,3- and 1,2-diols) of five-, six-, and seven-membered ring oxidizes much slower than the pro-*R*-configurated carbon center. Notably, the transition states are difficult to discern given the complexity of the polymer structures. Oxidation of **I** with H_2O_2 gives **II**.[64] Nanocluster Pd/Au-**17** provides excellent enantioselectivities (91 – 99% ee) in the oxidation of diols, and results of the enantioselectivity from the oxidation of *trans*-diols are comparable to those reported using enzymes.[65,66]

Catalytic asymmetric oxidation of alkenes.

The success in catalytic asymmetric oxidation of diols led us to examine the oxidation of alkenes. Although no oxidation of alkenes took place at 1 atmospheric of oxygen, various alkenes were readily oxidized at 30 psi. of oxygen in excellent to good chemical yields and excellent optical yields. Results of the oxidation are summarized in **Table 2** (entries 1 – 7). For example, treatment of 1,2-dihydronaphthalene (**37**) with 0.5 mol% of Pd/Au (3:1)-**17** in water at 25°C under 30 psi. of oxygen for 3 days gave (1*S*,2*R*)-**38** in 86% yield and 99% ee

Table 2. Catalytic asymmetric oxidation of alkenes and cycloalkanes.

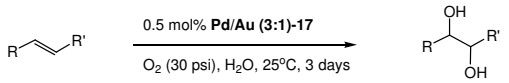

entry	substrate	product(s)	% yield(s)	% ee
1	**37**	(1*S*,2*R*)-**38**	86	99
2	**39**	(1*S*,2*S*)-**40** ; (1*R*,2*S*)-**41**	87 , 6	99 , 97
3	**39A**	(1*S*,2*R*)-**41A** ; (1*R*,2*R*)-**40A**	90 , 8	98 , 98
4[(a)]	**42**	(2*R*,3*S*)-**43** ; (2*R*,3*R*)-**44**	82 , 3	99 , 97
5[(a)]	**45**	(1*S*,2*R*)-**46** ; (1*R*,2R)-**47**	67 , 11	93 , 94
6[(b)]	**45**	(1*S*,2*R*)-**46** ; (1*R*,2R)-**47**	5 , 59	89 , 91
7[(c)]	(*R*)-**48**	(1*S*,2*R*,4*R*)-**49**	92	-

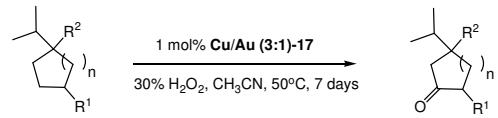

entry	substrate	product	% yield	% ee[(d)]
8	**50**	(2*R*,5*S*)-**51**	87	81
9	**52**	(*R*)-**55**	91	92
10	**53**	(*R*)-**56**	98	91
11	**54**	(*R*)-**57**	89	93
12	**58**	(*R*)-**59**	98	93
13	(+)-sclareolide (**60**)	**61**	38[(e)]	-

[(a)] Reactions were conducted at 50°C for 3 days; [(b)] reactions were conducted at 70°C for 5 h in the presence of 0.3 equiv K_2CO_3. No hydroxyindanones were detected; [(c)] a single stereoisomer was isolated and no other stereoisomers were detected; [(d)] percent ee's were determined by HPLC/chiral column using 220 nm wavelength for detection; [(e)] An 8 mol % of the catalyst were used at 60°C for 6 days, and a 46% of (+)-sclareolide (**60**) was recovered.

(**Table 2**, entry 1). Only a single product was obtained in the reaction. The Sharpless dihydroxylation of **37** using DP-PHAL gave 56% ee of (1*R*,2*S*) enantiomer of **38**.[67] Other disubstituted alkenes including *trans*- and *cis*-β-methylstyrene (**39** and **39A**, respectively; **Table 2**, entries 2 and 3) also underwent oxidation reactions at 25°C. In the oxidation of *trans*-**39**, the syn-adduct (1*S*,2*S*)-**40** was isolated in 87% yield and 99% ee along with a small amount of anti-adduct (1*R*,2*S*)-

41 in 6% yield and 97% ee. Similarly, in the oxidation of *cis*-**39A**, the syn-adduct (1*S*,2*R*)-**41A** was isolated in 90% yield and 98% ee as well as 8% yield of anti-adduct (1*R*,2*R*)-**40A** in 98% ee. Notably, the dihydroxylation takes place from the *re* face of the alkenes (in regarding to C1 of **37** or **39**). Trisubstituted alkenes such as (*R*)-(+)-limonene (**48**), containing a stereogenic center, also underwent stereoselective oxidation at 25°C to give a single stereoisomer (1*S*,2*R*,4*R*)-**49**. No other stereoisomers were detected. The oxidation of alkenes containing an electron-withdrawing group such as *trans*-cinnamic acid ester **42** and indene (**45**) only proceeded at 50°C giving the syn-adducts (2*R*,3*S*)-**43** (82% yield; 99% ee) and (1*S*,2*R*)-**46** (67% yield; 93% ee), respectively, as the major products. The respective anti-adducts, (2*R*,3*R*)-**44** (3% yield; 97% ee) and (1*R*,2*R*)-**47** (11% yield; 94% ee) were also isolated as minor products. Since (1*R*,2*R*)-**47** was obtained in 11% yield, we questioned whether this anti-adduct could be produced as the major product. As expected, in the presence of 0.3 equiv of K_2CO_3 at 70°C for 5 h, (1*R*,2*R*)-**47** was isolated in 59% yield and 91% ee. However, only syn-addut (1*S*,2*R*)-**38** was isolated when 0.3 equiv of K_2CO_3 was added to the oxidation reaction of **37** at 25°C. The absolute configurations were determined by comparing the sign and specific rotations of the respective reported molecules (see SI).[65,66,68,69] Optical purities of all dihydroxylated molecules were measured using HPLC/chiral column (SI). To determine the stereochemistry of **49** (which has not been reported previously), we independently prepared (1*S*,2*R*,4*R*)-**49** and its (1*R*,2*S*,4*R*)-diastereomer by the reaction of (*R*)-**48** with OsO_4 (catalytic amount)-NMO followed by silica gel column chromatography (SI). The cyclic trisubstituted alkene reacted preferentially compared to the acyclic terminal disubstituted olefin group, suggesting electron-donating groups such as alkyl and aryl enhance the reactivity towards the nanoclusters. The formation of (1*S*,2*R*,4*R*)-**49** from the dihydroxylation reaction of limonene is remarkable, since the

Scheme 3. Proposed mechanism and stereo- and regio-chemistry of the enantioselective oxidation of alkenes.

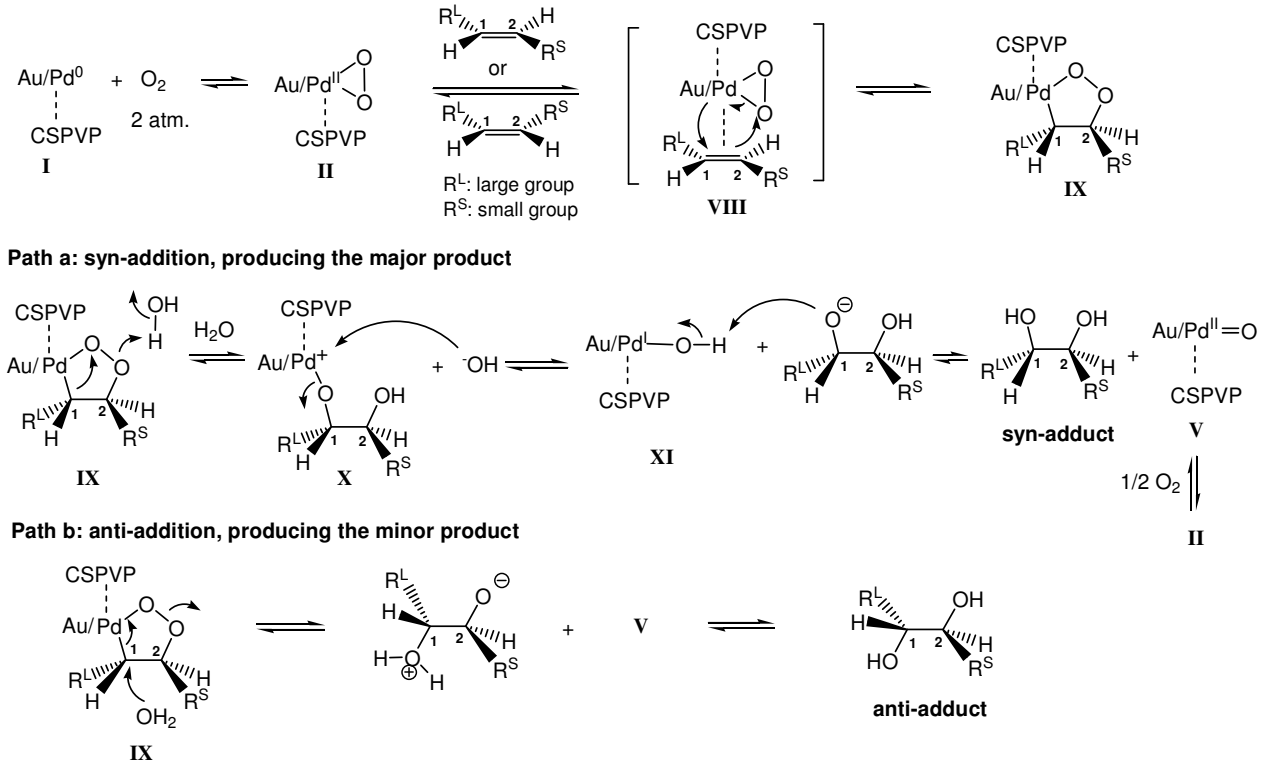

Stereo- and regio-chemistry of the oxidation of benzocycloalkenes, trisubstituted cycloalkenes (*R*-limonene), *trans*- and *cis*-alkenes:

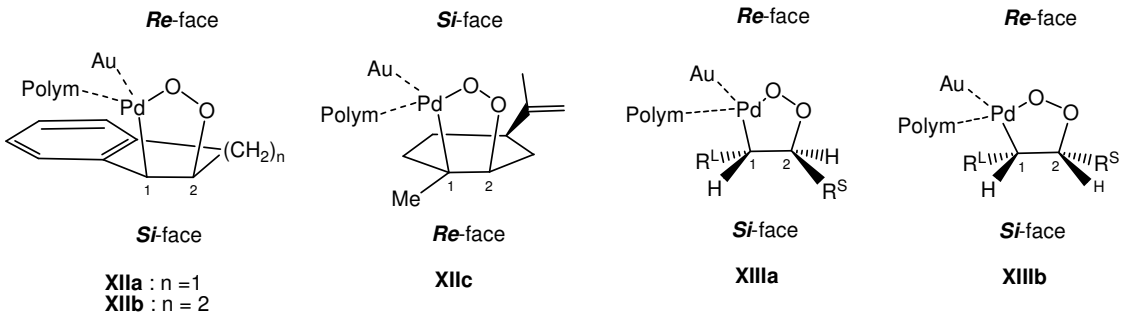

dihydroxyl functions were delivered from the same side of the bulky isopropenyl group. The highest reported % ee's of the dihydroxylation products of **39**, **39A**, **42** (the ethyl ester analog), and **45** from Sharpless asymmetric dihydroxylation reactions are 98,[70] 81,[71] 99,[69] and 89,[72] respectively. Hence, the

Pd/Au-**17** provided higher or similar enantiomeric selectivities in the catalytic asymmetric dihydroxylation reactions.

A proposed mechanism and stereo- and regio-chemistry for the enantioselective oxidation of alkenes[62,73] are depicted in Scheme 3. Similar to that described in Scheme 2, η^2-peroxido Pd^{II} (peroxopalladium) species **II** undergoes syn-addition reaction with alkenes via transition state **VIII** under high oxygen pressure, where Pd adds to C1 containing larger aryl or alkyl group (R^L) and oxygen adds to C2 containing smaller alkyl group (R^S), resulting in metallo-1,2-dioxolane **IX**.[63] C1 containing either an aromatic ring (entries 1 – 6) or more substituted carbon (entry 7) is better able to accommodate the partial positive charge in the transition state (*vide infra*). Carbon-1 of **IX** undergoes a 1,2-alkyl shift from Pd to oxygen (path a) leading to intermediate **X**, which hydrolyzes to give the syn-adducts. In **37** and (*R*)-**48** (**Table 2**, entries 1 and 7), the 1,2-alkyl shift takes place rapidly and only the syn-adducts were found. In other investigated alkenes (**39** – **45**), in addition to major path a, water attacks C1 of intermediate **IX** from the backside, path b, providing anti-addition diols as the minor products (**Table 2**, entries 2 – 5). In supporting this hypothesis, an addition of 0.3 equiv. of K_2CO_3, a stronger nucleophile than water, resulted in the formation of anti-adduct (1*R*,2*R*)-**47** being the major product (**Table 2**, entry 6). Structures of the respective metallo-1,2-dioxolanes derived from the oxidation of benzocycloalkenes, *trans*- and *cis*-alkenes are depicted in **XIIa**, **XIIb**, **XIIIa**, and **XIIIb**, which resulted from the addition reactions of η^2-peroxido Pd^{II} from the *Re*-face of the alkenes. For trisubstituted alkene such as (*R*)-limonene, the addition took place from the *Si*-face (structure **XIIc**).

The asymmetric aerobic oxidation of alkenes by Pd/Au-**17** at ambient temperature or 50°C provided excellent chemical and optical yields of the syn-dihydroxylated products and in certain cases where higher temperature (such as 70°C) is required, an addition of a weak base such as K_2CO_3 afforded anti-dihydroxylated molecules as the major products.

Catalytic asymmetric oxidation of alkanes.

To explore the scope of the oxidation reactions, a more challenging catalytic asymmetric C-H oxidation was investigated. We found that Cu/Au (3:1)-**17** provided greater chemical and optical yields in C-H oxidation than Pd/Au (3:1)-**17**. Results of the catalytic asymmetric C-H oxidation reactions of various substituted achiral cycloalkanes using 1 mol% Cu/Au (3:1)-**17** and H_2O_2 at 50°C are summarized in **Table 2**. Without hydrogen peroxide, under oxygen atmosphere (30 psi.), no oxidation products were detected. For example, oxidation of meso-*trans*-1,4-diisopropylcyclohexane (**50**) gave an 87% yield of (2*R*,5*S*)-**51** in 81% ee (**Table 2**, entry 8). The specific rotation and ^{1}H and ^{13}C NMR spectral data of (2*R*,5*S*)-**51** were in agreement with those of the reported compound synthesized from (*S*)-perillaldehyde.[74] The four methine C-H's of **50**, possessing weaker bond dissociation energies,[31] and four sterically less hindered methyls were not oxidized under the reaction conditions, suggesting rigid or less freely rotated methylene groups are oxidized faster than methine and methyl groups. Higher ee's were obtained when a directing group such as hydroxyl was presented. Hence, oxidation of alcohols **52** - **54**, and 1-isopropenylcyclohexanol (**58**) gave excellent chemical and optical yields of (*R*)-**55** - (*R*)-**57**, and (*R*)-**59**,

Scheme 4. Proposed mechanism and oxidative sites of the enantioselective catalytic oxidation of alkanes.

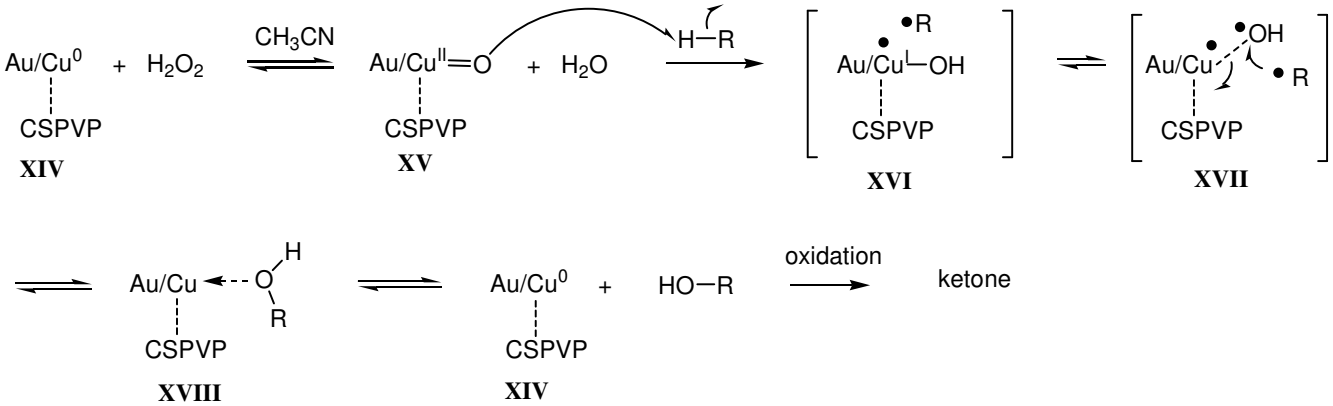

Stereo- and regio-chemistry of the major oxidative sites in the enantioselective catalytic C-H oxidation reactions:

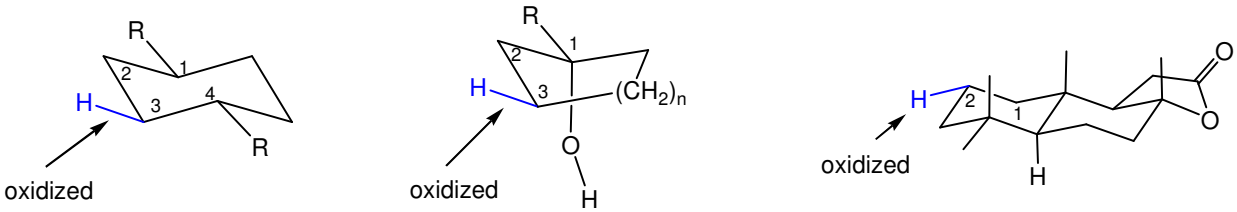

XIX (R = *i*-Pr) **XX** (R = *i*-Pr, isopropenyl; n = 1 = 3) **XXI**

respectively (**Table 2**, entries 9 – 12). Likely, under the reaction conditions, the alcohols were initially formed and they subsequently oxidized to the ketones. Importantly, in the absence of elevated pressure of oxygen, the alkene function of **58** was not oxidized at 50°C, despite the presence of an activating allylic hydroxyl group. This is significant since alkene functional group is more reactive than the alkane moiety. The regiochemistry of (*R*)-**55** - (*R*)-**57**, and (*R*)-**59** were analyzed by 2D COSY spectroscopy. In the COSY spectrum of (*R*)-**55**, the signal at δ 2.41 – 2.30 ppm assigned for C2-hydrogens has no correlation with other protons, while the signals at ~2.25 and 2.05 ppm assigned for C5 hydrogens show correlation with C4 hydrogens at 2.01 and 1.60 ppm. Similar correlations were found in the 2D COSY spectra of (*R*)-**56**, (*R*)-**57**, and (*R*)-**59** (SI). Moreover, (*R*)-**56** and (*R*)-**57** were independently synthesized from (*S*)-**23** and (*S*)-**24**, respectively, by silylation of the C3-hydroxyl group followed by addition reaction with isopropylmagnesium bromide, removal of the silicon protecting group, and oxidation with IBX-DMSO (see SI). Their NMR spectra and specific rotations were similar to those obtained from the C-H oxidations. A medium-sized natural product, (+)-sclareolide (**60**), also underwent regioselective oxidation to give 2*S*-2-hydroxysclareolide (**61**) in 38% yield and 3% yield of 1-oxosclareolide along with 46% recovery of **60** after silica gel column chromatographic separation. No other regioisomers were found. ^{1}H and ^{13}C NMR spectral data of **61** and 1-oxosclareolide are identical to those reported.[75,34] Notably, unlike the reported iron complex-catalyzed oxidation,[34] the C2-equatorial hydroxyl function of **61** does not undergo further oxidation, likely due to steric hindrance (C2-axial-H is shielded by C15-β- and C16-methyls[75]).

Based on the previously suggested mechanism of copper complexes bearing trispyrazolylborate ligands,[76] a mechanism for the C-H oxidation reactions involving Cu/Au-**17** was proposed and the stereo- and regio-chemistry of the major C-H oxidative sites were depicted in Scheme 4. Cu°/Au **XIV** reacts with H_2O_2 to give copper(II) oxo complex **XV**, which abstracts a hydrogen atom from cycloalkanes such as **50** to generate hydroxyl copper(I) and cycloalkyl radical (likely not a free radical[76]) in a cage-like complex **XVI**. A rapid combination of the cycloalkyl radical with hydroxyl radical in **XVII** takes place and subsequently releases the alcohol and regenerates **XIV**. The alcohols oxidized under the reaction conditions to give ketones.[76] Oxidative sites for the C-H oxidation reactions are summarized in **XIX** - **XXI**. The two isopropyl substituents orient at the equatorial positions and copper(II) oxo **XV** likely approaches the C3 equatorial hydrogen, resulting in the observed 2*R*,5*S* configuration in **51**. In the hydroxyl directed oxidation, C1 hydroxyl group coordinates with copper(II) oxo **XV** and abstraction of the C3 equatorial or axial hydrogen will lead to the observed C3-*R* configuration.

CONCLUSION.

Various substituted poly-*N*-vinylpyrrolidinones containing a stereogenic center were synthesized from L-amino acids and used in the catalytic asymmetric oxidations of cyclic diols, dihydroxylation of alkenes, and C-H oxidation of cycloalkanes. Polymer **17** afforded the highest enantiomeric selectivities. Excellent chemical yields and enantioselectivity were found. Both (±)-*trans* and meso-*cis* diols were oxidized under oxygen atmosphere with Pd/Au-CSPVP to give (*S*)-hydroxy ketones. *Trans*- and *cis*-alkenes oxidized under 30 psi. of oxygen to afford *syn*-diols as the major products. The resulting diols do not undergo further oxidation. Various substituted cycloalkanes including 1,4-disubstituted cyclohexane and 1-substituted 1-cycloalkanols were oxidized by Cu/Au-**17** and H_2O_2 to furnish chiral cycloalkanones. Remarkably, disubstituted terminal alkene function was not oxidized under the C-H oxidation reaction conditions, which demonstrates a high potential for the synthetic methodology.

ASSOCIATED CONTENT

Supporting Information. Molecular weight determination, ICP-MS, TEM, AFM and DLS images, XPS spectra, experimental procedures, HPLC/chiral column graphs, ^{1}H and ^{13}C NMR spectra of the described molecules, and 2D COSY spectra. This material is available free of charge via the Internet at http://pubs.acs.org.

AUTHOR INFORMATION

Corresponding Author

* duy@ksu.edu

Present Addresses

†S.N.S. and V.N.: Department of Chemistry, Regis University, Denver, CO.

Author Contributions

The manuscript was written through contributions of all authors. All authors have given approval to the final version of the manuscript.

Notes

The authors declare no competing financial interest.

ACKNOWLEDGMENT

We thank Johnson Cancer Research Center, Kansas State University for partial support of this project, NIH National Institute of General Medical Sciences (P20 GM103418) for supporting A.M., NSF REU program (CHE1460898) for supporting V.N., and SUROP program, Kansas State University for supporting S.N.S. of a summer research program. D.H.H. thanks the Japan Society for the Promotion of Science (ID No. L14527) for a Visiting Professorship at the Institute for Molecular Science and Osaka University, Japan. We thank Professor Hidehiro Sakurai and Ms. Setsiri Haesuwannakij for helpful discussion and analysis of initial nanoclusters, and Dr. Hongwang Wang and Prof. Christopher Sorensen for assisting B.H. in obtaining and discussion of DLS data, respectively.

ABBREVIATIONS

AFM, atomic force microscopy; AIBN, azobisisobutyronitrile; Au, gold; COSY, correlation spectroscopy; CSPVP, chiral substituted poly-*N*-vinylpyrrolidinone; Cu, copper; DLS, dynamic light scattering; IBX, 2-iodoxybenzoic acid; ICP-MS, inductively coupled plasma-mass spectrometry; NMO, *N*-methylmorpholine *N*-oxide; PAMAM, poly(amidoamine); Pd, palladium; PVP, poly-*N*-vinylpyrrolidinone; TEM, transmission electron microscopy; TFA, trifluoroacetic acid; XPS, X-ray photoelectron spectroscopy.

REFERENCES

1. Zhang, H.; Watanabe, T.; Okumura, M.; Haruta, M.; Toshima, N. *Nature Mater*. **2012**, *11*, 49.
2. Miyamura, H.; Kobayashi, S. *Acc. Chem. Res*. **2014**, *47*, 1054.
3. Hou, W.; Dehm, N. A.; Scott, R. W. J. *J. Catal*. **2008**, *253*, 22.

4. Toshima, N.; Yonezawa, T. *New J. Chem*. **1998**, *22*, 1179.
5. Yao, H.; Kobayashi, R. *Colloid Interface Sci*. **2014**, *419,* 1.
6. Kanaoka, S.; Yagi, N.; Fukuyama, Y.; Aoshima, S.; Tsunoyama, H.; Tsukuda, T.; Sakurai, H. *J. Am. Chem. Soc*. **2007**, *129,* 12060.
7. Sophiphun, O.; Wittayakun, J.; Dhital, R. N.; Haesuwannakij, S.; Murugadoss, A.; Sakurai, H. *Aust. J. Chem*. **2012**, *65*, 1238.
8. Lu, J.; Toy, P. H. *Chem. Rev*. **2009**, *109,* 815.
9. Deng, D.; Jin, Y.; Cheng, Y.; Qi, T.; Xiao, F. *ACS Appl. Mater. Interfaces* **2013**, **5**, 3839.
10. Zhang, H.; Toshima, N. *J. Nanosci. & Nanotechnol.* **2013**, *13,* 5405.
11. Nishimura, S.; Yakita, Y.; Katayama, M.; Higashimine, K.; Ebitani, K. *Catal. Sci. & Technol*. **2013**, *3,* 351.
12. Zhang, S.; Shao, Y.; Liao, H.; Liu, J.; Aksay, I. A.; Yin, G.; Lin, Y. *Chem Mater*. **2011**, *23,* 1079.
13. Wang, F.; Jiang, Y.; Wen, X.; Xia, J.; Sha, G.; Amal, R. *ChemCatChem* **2013**, *5,* 3557.
14. Murugadoss, A.; Okumura, K.; Sakurai, H. *J. Phys. Chem. C* **2012**, *116,* 26776.
15. Dhital, R. N.; Kamonsatikul, C.; Somsook, E.; Bobuatong, K.; Ehara, M.; Kranjit, S.; Sakurai, H. *J. Am. Chem. Soc*. **2012**, *134,* 20250.
16. Dhital, R. N.; Sakurai, H. *Chem. Lett*. **2012**, *41,* 630.
17. Yoo, W. –J.; Miyamura, H.; Kobayashi, S. *J. Am. Chem. Soc*. **2011**, *133,* 3095.
18. Suzuki, T. Desymmetrization of meso diols. Yamamoto, H.; Carreira, E., Eds. Comprehensive chirality, Elsevier: Amsterdam, 2012, volume 5 (21), page 502-533.
19. Meng, S. –S.; Liang, Y.; Cao, K. –S.; Zou, L.; Lin, X. –B.; Yang, H.; Houk, K. N.; Zheng, W. –H. *J. Am. Chem. Soc*. **2014**, *136*, 12249.
20. Moritani, J.; Hasegawa, Y.; Kayaki, Y.; Ikariya, T. *Tetrahedron Lett*. **2014**, *55*, 1188.
21. Mandal, S. K.; Jensen, D. R.; Pugsley, J. S.; Sigman, M. S. *J. Org. Chem*. **2003**, *68*, 4600.
22. Jakka, K. & Zhao, C. –G. *Org. Lett*. **2006**, *8*, 3013.
23. Noe, M.C.; Letavic, M.A.; Snow, S. L. Asymmetric dihydroxylation of alkenes. Organic Reactions; Overman, L. E. Ed., John Wiley & Sons: Hoboken, New Jersey, 2005, Vol. 66, 109-625.
24. Konieczny, S.; Leurs, M.; Tiller, J. C. *ChemBioChem* **2015**, *16*, 83.
25. Shilpa, N.; Manna, J.; Rana, R. K. *Eur. J. Inorg. Chem*. **2015**, *29*, 4965.
26. Bataille, C. R.; Donohoe, T. J. *Chem. Soc. Rev*. **2011**, *40*, 114.
27. Stoltz, B. M. *Chem. Lett*. **2004**, *33*, 362.
28. Neisius, N. M.; Plietker, B. *J. Org. Chem*. **2008**, *73*, 3218.
29. de Boer, J. W.; Browne, W. R.; Harutyunyan, S. R.; Bini, L.; Tiemersma-Wegman, T. D.; Alsters, P. L.; Hage, R.; Feringa, B. L. *Chem. Commun*. **2008**, 3747.
30. Zhang, C.; Liu, Y.; Xu, Z. –J.; Tse, C. –W.; Guan, X.; Wei, J.; Huang, J. –S.; Che, C. –M. *Angew. Chem. Int. Ed*. **2016**, *55*, 10253.
31. Newhouse, T.; Baran, P. S. *Angew. Chem. Int. Ed*. **2011**, *50*, 3362.
32. Gormisky, P. E.; White, M. C. *J. Am. Chem. Soc*. **2013**, *135*, 14052.
33. Osberger, T. J.; Rogness, D. C.; Kohrt, J. T.; Stepan, A. F.; White, M. C. *Nature* **2016**, *537*, 214.
34. Canta, M.; Font, D.; Gomez, L.; Ribas, X.; Costas, M. *Adv. Synth. Catal*. **2014**, *356*, 818.
35. Boorman, T. C.; Larrosa, I. *Chem. Soc. Rev*. **2011**, *40*, 1910.
36. Gutekunst, W. R.; Baran, P. S. *Chem. Soc. Rev*. **2011**, *40*, 1976.
37. Lu, H.; Zhang, X. P. *Chem. Soc. Rev*. **2011**, *40*, 1899.
38. Collet, F.; Lescot, C.; Dauban, P. *Chem. Soc. Rev*. **2011**, *40*, 1926.
39. Covell, D. J.; White, M. C. *Angew. Chem. Int. Ed*. **2008**, *47*, 6448.
40. Hoke, T.; Herdtweck, E.; Bach, T. *Chem. Commun*. **2013**, *49*, 8009.
41. Wei, X. –H.; Wang, G. –W.; Yang, S. –D. *Chem. Commun*. **2015**, *51*, 832.
42. Liu, Y.; Tsunoyama, H.; Akita, T.; Xie, S.; Tsukuda, T. *ACS Catal*. **2011**, *1*, 2.
43. Rekkab-Hammoumraoui, I.; Choukchou-Braham, A.; Pirault-Roy, L.; Kappenstein, C. *Bull. Mater. Sci*. **2011**, *34*, 1127.
44. Weir, M. G.; Knecht, M. R.; Frenkel, A. I.; Crooks, R. M. Langmuir **2010**, *26*, 1137.
45. Smrcina, M.; Majer, P.; Majerova, E.; Guerassina, T. A.; Eissenstat, M. A. *Tetrahedron* **1997**, *53*, 12867.
46. Kerr, M. S.; de Alaniz, J. R.; Rovis, T. *J. Org. Chem*. **2005**, *70*, 5725.
47. Ward, B. D.; Risler, H.; Weitershaus, K.; Bellemin-Laponnaz, S.; Wadepohl, H.; Gade, L. H. *Inorg. Chem*. **2006**, *45*, 7777.
48. Digenis, G. A.; McClannahan, J. S.; Chen, P. –L. *J. Labelled Comp. Radiopharm*. **1993**, *33*, 11.
49. Kawaguchi, S.; Ito, K. *Adv. Polym. Sci*. **2005**, *175*, 299.
50. Zhai, L.; Shi, T.; Wang, H. *Front. Chem. China* **2009**, *4*, 83.
51. Flebbe, T.; Hentschke, R.; Hadicke, E.; Schade, C. *Macromol. Theory Simul*. **1998**, *7*, 567.
52. Ferrando, R.; Jellinek, J.; Johnston, R. L. *Chem. Rev*. **2008**, *108*, 850.
53. Mulvaney, P.; Giersig, M. *J. Chem. Soc., Faraday Trans.* **1996**, *92*, 3137.
54. Poole, C. P. Jr.; Owens, F. J. Introduction to Nanotechnology; John Wiley & Sons: New Jersey, 2003. Pages 12 - 15.
55. Kobayashi, S.; Xu, P.; Endo, T.; Ueno, M.; Kitanosono, T. *Angew. Chem. Int. Ed*. **2012**, *51*, 12763.
56. Chen, B. –S.; Hanefeld, U. *J. Mol. Catal. B: Enz*. **2013**, *85-86*, 239.
57. Lifchits, O.; Mahlau, M.; Reisinger, C. M.; Lee, A.; Fares, C.; Plyak, I.; Gopakumar, G.; Thiel, W.; List, B. *J. Am. Chem. Soc*. **2013**, *135*, 6677-6693.
58. Zhang, J.; Xu, T.; Li, Z. *Adv. Synth. Catal*. **2013**, *355*, 3147.
59. Liu, Y.; Li, R. –R.; Lu, X. –B. *Macromol.* **2015**, *48*, 6941.
60. Singh, G.; Aube, J. *Org. Biomol. Chem*. **2016**, *14*, 4299.
61. Lehtonen, A.; Kivekas, R.; Sillanpaa, R. *Polyhedron* **2002**, *21*, 1133.
62. Stahl, S. S., Thorman, J. L., Nelson, R. C.; Kozee, M. A. *J. Am. Chem. Soc*. **2001**, *123*, 7188.
63. Stahl, S. S. *Angew. Chem. Int. Ed*. **2004**, *43*, 3400.
64. Talsi, E. P.; Bryliakov, K. P. *Coord. Chem. Rev*. **2012**, *256*, 1418.
65. Boyd, D. R.; Sharma, N. D.; Berberian, M. V.; Cleij, M.; Hardacre, C.; Ljubez, V.; McConville, G.; Stevenson, P. J.; Kulakov, L. A.; Christopher, C. R. A. *Adv. Synth. Catal*. **2015**, *357*, 1881.
66. Kihumbu, D.; Stillger, T.; Hummel, W.; Liese, A. *Tetrahedron: Asym*. **2002**, *13*, 1069.
67. Becker, H.; King, S. B.; Taniguchi, M.; Vanjesscje, P. M.; Sharpless, K. B. *J. Org. Chem*. **1995**, *60*, 3940.
68. Jin, Y.; Yao, Z.; Zhang, S.; Jiang, R.; Sun, X. *Chinese J. Org. Chem*. **2007**, *27*, 602.
69. Sengupta, S.; Mondal, S. *Tetrahedron Lett*. **1999**, *40*, 3469.
70. Ahrgren, L.; Sutin, L. *Org. Proc. Res. Dev*. **1997**, *1*, 425.
71. Fuji, K.; Tanaka, K.; Miyamoto, H. *Tetrahedron Lett*. **1992**, *33*, 4021.
72. Reddy, S. M.; Srinivasulu, M.; Reddy, Y. V.; Narasimhulu, M.; Venkateswarlu, Y. *Tetrahedron Lett*. **2006**, *47*, 5285.
73. Wu, W.; Jiang, H. *Acc. Chem. Res*. **2012**, *45*, 1736.
74. Pisoni, D. d. S.; da Costa, J. S.; Gamba, D.; Petzhold, C. L.; Borges, A. C. de A.; Ceschi, M. A.; Lunardi, P.; Goncalves, C. A. S. *Eur. J. Med. Chem*. **2010**, *45*, 526.
75. Choudhary, M. I.; Musharraf, S. G.; Sami, A.; Raman, A. –u. *Helv. Chim. Acta* **2004**, *87*, 2685.
76. Conde, A., Vilella, L., Balcells, D., Diaz-Requejo, M. M., Lledos, A.; Perez, P. J. *J. Am. Chem. Soc*. **2013**, *135*, 3887.

For TOC Only

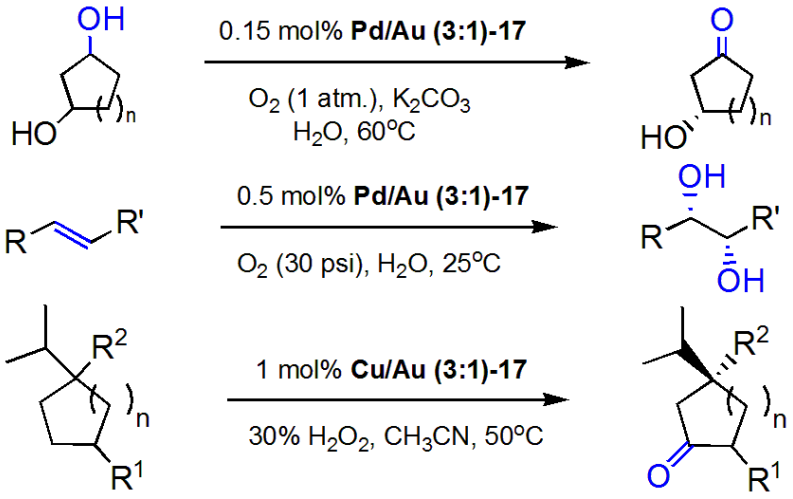
OH
HO
n
0.15 mol% Pd/Au (3:1)-17
O2 (1 atm.), K2CO3
H2O, 60°C
O
HO
n
R
R'
0.5 mol% Pd/Au (3:1)-17
O2 (30 psi), H2O, 25°C
OH
R
R'
OH
R2
n
R1
1 mol% Cu/Au (3:1)-17
30% H2O2, CH3CN, 50°C
R2
n
O
R1

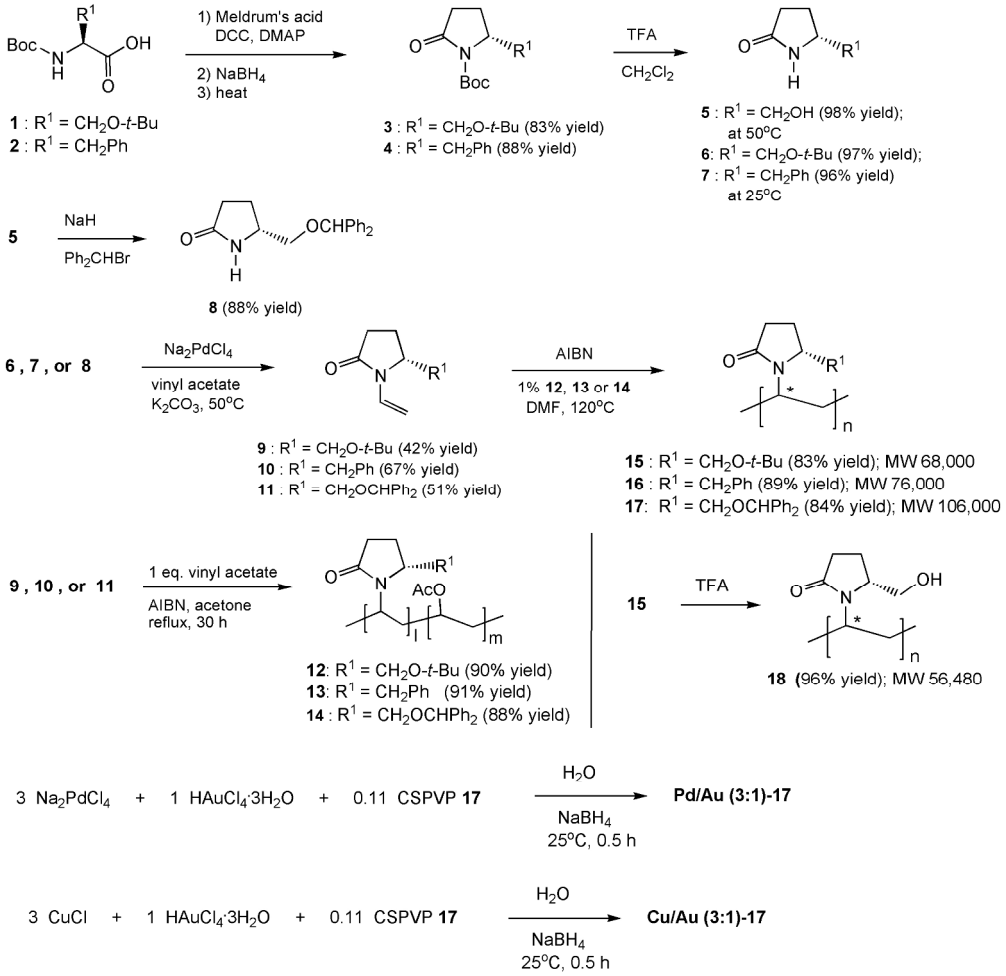

241x235mm (300 x 300 DPI)

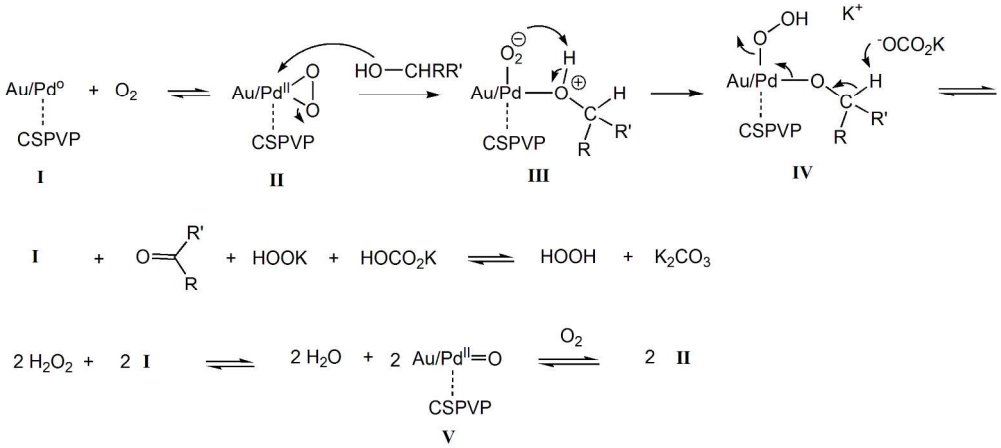

Oxidative sites for racemic **1,3- and 1,2-*trans*-diols** leading to (*S*)-hydroxy ketones:

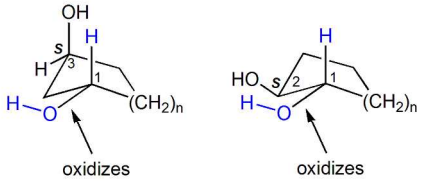

VIa (n = 1 - 3) **VIb** (n = 1 - 3)

Oxidative sites for meso **1,3- and 1,2-*cis*-diols** leading to (*S*)-hydroxy ketones:

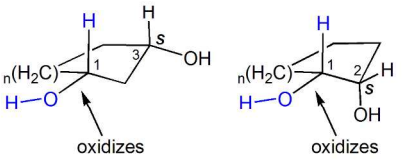

VIIa (n = 1 - 3) **VIIb** (n = 1 - 3)

226x174mm (300 x 300 DPI)

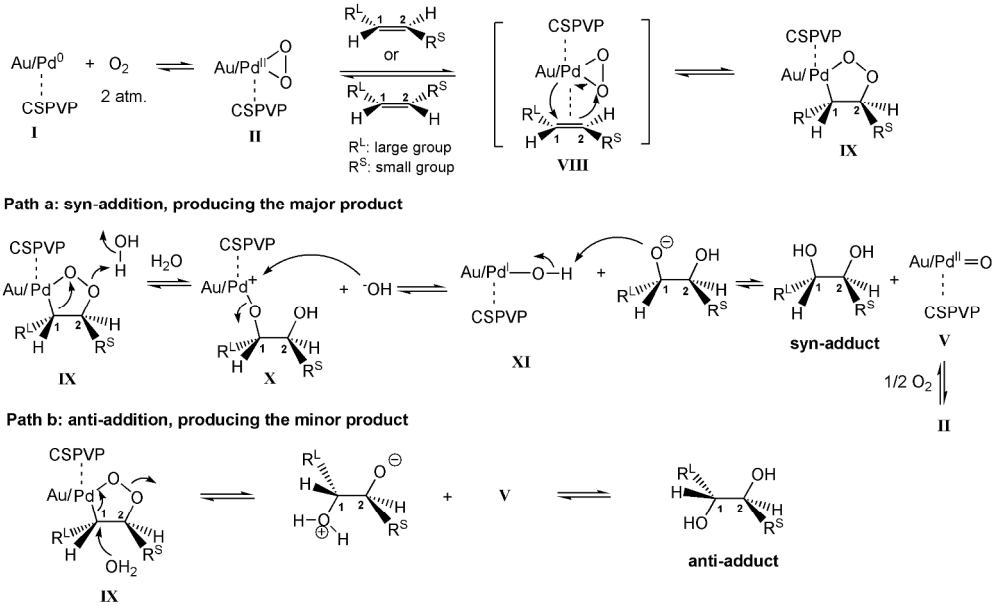

Stereo- and regio-chemistry of the oxidation of benzocycloalkenes, trisubstituted cycloalkenes (*R*-limonene), *trans*- and *cis*-alkenes:

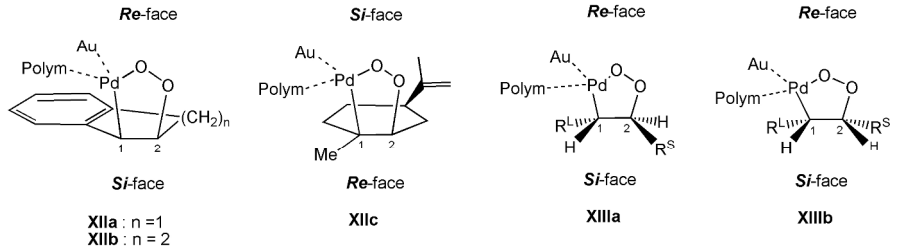

252x232mm (300 x 300 DPI)

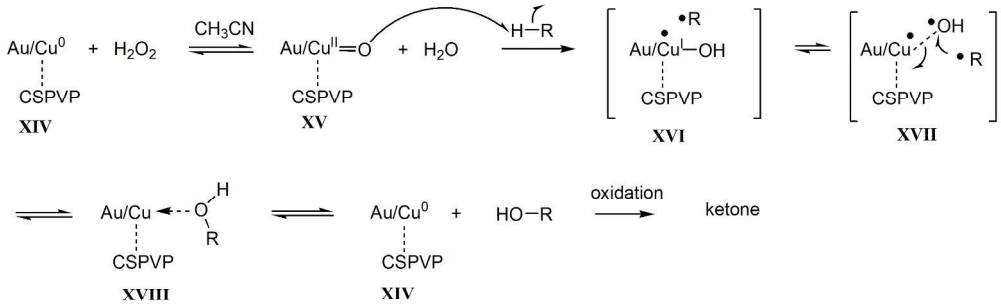

Stereo- and regio-chemistry of the major oxidative sites in the enantioselective catalytic C-H oxidation reactions:

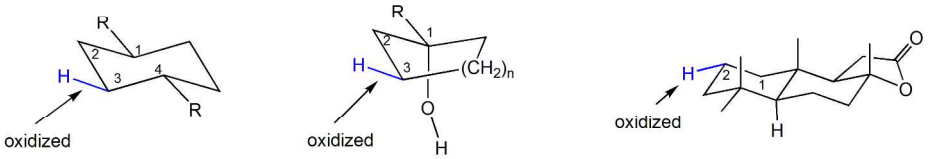

XIX (R = *i*-Pr) **XX** (R = *i*-Pr, isopropenyl; n = 1 = 3) **XXI**

232x139mm (300 x 300 DPI)

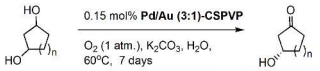

entry	substrate	CSPVP	product	% yield[a]	% ee	recovered diol	% yield[b]	% ee
1	(±)-**20**	**15**	(S)-**23**	46	83	(*R*,*R*)-**20**	52	79
2	(±)-**20**	**16**	(S)-**23**	47	88	(*R*,*R*)-**20**	52	81
3	(±)-**20**	**17**	(S)-**23**	49	99	(*R*,*R*)-**20**	50	92
4	(±)-**20**	**18**	(S)-**23**	46	70	(*R*,*R*)-**20**	51	65
5	(±)-**19**	**17**	(*S*)-**22**	48	99	(*R*,*R*)-**19**	53	91
6	(±)-**21**	**17**	(*S*)-**24**	46	99	(*R*,*R*)-**21**	53	85
7[c]	**25**	**17**	(*S*)-**22**	97	90	-	-	-
8[c]	**26**	**17**	(S)-**23**	89	91	-	-	-
9[c]	**27**	**17**	(*S*)-**24**	95	92	-	-	-

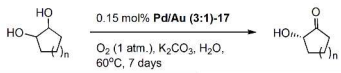

entry	substrate	CSPVP	product	% yield[a]	% ee	recovered diol	% yield[b]	% ee
10	(±)-**28**	**17**	(*S*)-**31**	47	99	(*R*,*R*)-**28**	50	88
11	(±)-**29**	**17**	(S)-**32**	45	99	(*R*,*R*)-**29**	50	87
12	(±)-**30**	**17**	(*S*)-**33**	47	99	(*R*,*R*)-**30**	54	88
13[c]	**34**	**17**	(*S*)-**31**	94	91	-	-	-
14[c]	**35**	**17**	(S)-**32**	97	92	-	-	-
15[c]	**36**	**17**	(*S*)-**33**	94	91	-	-	-

372x246mm (300 x 300 DPI)

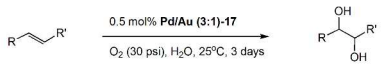

entry	substrate	product(s)	% yield(s)	% ee
1	**37**	(1*S*,2*R*)-**38**	86	99
2	**39**	(1*S*,2*S*)-**40** (1*R*,2*S*)-**41**	87 , 6	99 , 97
3	**39A**	(1*S*,2*R*)-**41A** (1*R*,2*R*)-**40A**	90 , 8	98 , 98
4[a]	**42**	(2*R*,3*S*)-**43** (2*R*,3*R*)-**44**	82 , 3	99 , 97
5[a]	**45**	(1*S*,2*R*)-**46** (1*R*,2R)-**47**	67 , 11	93 , 94
6[b]	**45**	(1*S*,2*R*)-**46** (1*R*,2R)-**47**	5 , 59	89 , 91
7[c]	(*R*)-**48**	(1*S*,2*R*,4*R*)-**49**	92	-

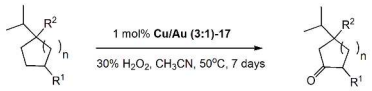

entry	substrate	product	% yield	% ee[d]
8	**50**	(2*R*,5*S*)-**51**	87	81
9	**52**	(*R*)-**55**	91	92
10	**53**	(*R*)-**56**	98	91
11	**54**	(*R*)-**57**	89	93
12	**58**	(*R*)-**59**	98	93
13	(+)-sclareolide (**60**)	**61**	38[e]	-

371x279mm (300 x 300 DPI)

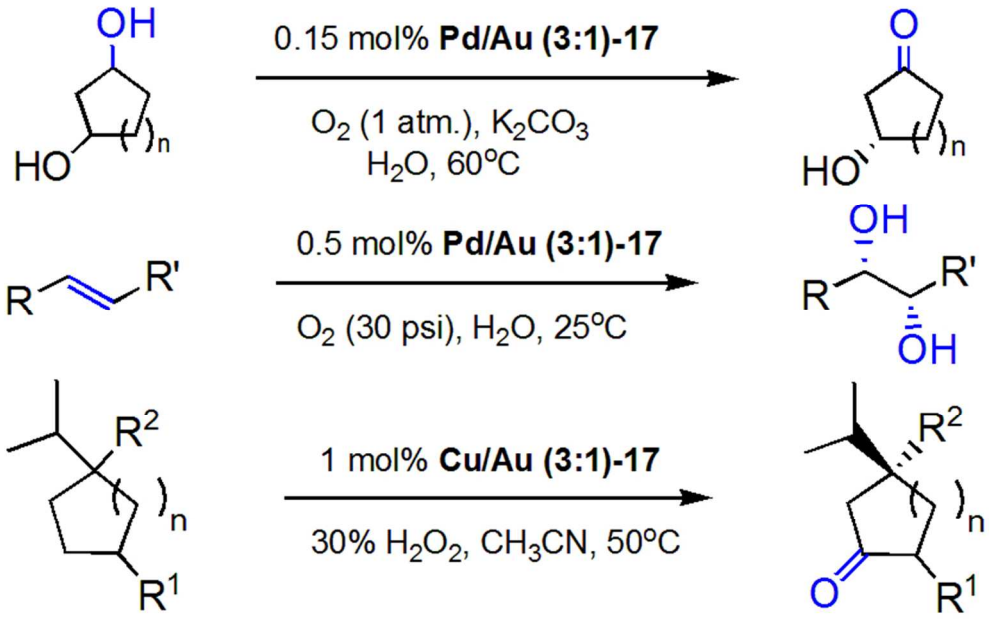

71x44mm (300 x 300 DPI)